UNCLASSIFIED

AD NUMBER
ADB111121
LIMITATION CHANGES

TO:

Approved for public release; distribution is unlimited.

FROM:

Distribution authorized to U.S. Gov't. agencies and their contractors; Critical Technology; MAR 1987. Other requests shall be referred to Air Force Rocket Propulsion Laboratory, Edward AFB, CA 93523-5000. This document contains export-controlled technical data.

AUTHORITY

AFRPL per ltr, 20 Mar 1997

THIS PAGE IS UNCLASSIFIED

AFRPL TR-85-096

AD:

Interim Report
for the period
May 1985 to
September 1985

Solar Plasma Propulsion

DTIC
S ELECTE D
MAY 1 1 1987
D

March 1987

Author:
C. W. Larson

University of Dayton Research Institute
300 College Park, KL 465
Dayton, OH 45469

UDR-TR-117
F04611-83-C-0046

AD-B111 121

prepared for the: **Air Force
Rocket Propulsion
Laboratory**

Air Force Space Technology Center
Space Division, Air Force Systems Command
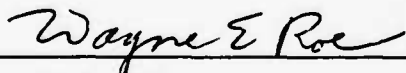Edwards Air Force Base,
California 93523-5000

87 5 8 054

WAYNE E. ROE
RESEARCH COORDINATOR

FRANKLIN B. MEAD
TASK MANAGER

FOR THE COMMANDER

JAMES. T. EDWARDS
CHIEF, PLANS AND PROGRAMS

CLARK W. HAWK
DIVISION CHIEF

REPORT DOCUMENTATION PAGE

1a. REPORT SECURITY CLASSIFICATION		1b. RESTRICTIVE MARKINGS
Unclassified		N/A 611121h

2a. SECURITY CLASSIFICATION AUTHORITY	3. DISTRIBUTION/AVAILABILITY OF REPORT
N/A	Distribution authorized to U.S. Government agencies and their contractors;
2b. DECLASSIFICATION/DOWNGRADING SCHEDULE	Critical Technology, (see reverse)
N/A	

4. PERFORMING ORGANIZATION REPORT NUMBER(S)	5. MONITORING ORGANIZATION REPORT NUMBER(S)
UDR-TR-85-117	AFRPL-TR-85-096

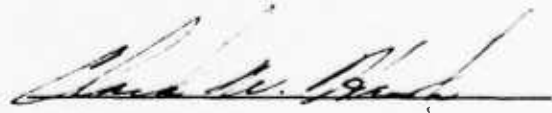| 6a. NAME OF PERFORMING ORGANIZATION	6b. OFFICE SYMBOL (If applicable)	7a. NAME OF MONITORING ORGANIZATION
University of Dayton Research Institute		Air Force Rocket Propulsion Laboratory

6c. ADDRESS (City, State and ZIP Code)	7b. ADDRESS (City, State and ZIP Code)
300 College Park KL 465 Dayton, OH 45469	Edwards Air Force Base, CA 93523-5000

8a. NAME OF FUNDING/SPONSORING ORGANIZATION	8b. OFFICE SYMBOL (If applicable)	9. PROCUREMENT INSTRUMENT IDENTIFICATION NUMBER
		F04611-83-C-0046

8c. ADDRESS (City, State and ZIP Code)	10. SOURCE OF FUNDING NOS.			
	PROGRAM ELEMENT NO.	PROJECT NO.	TASK NO.	WORK UNIT NO.
	61102 F	2308	M3	RI

11. TITLE (Include Security Classification)
Solar Plasma Propulsion

12. PERSONAL AUTHOR(S)
Larson, C. W., Ph.D.

13a. TYPE OF REPORT	13b. TIME COVERED	14. DATE OF REPORT (Yr., Mo., Day)	15. PAGE COUNT
Interim	FROM 85/5 TO 85/9	87/3	29

16. SUPPLEMENTARY NOTATION

17. COSATI CODES			18. SUBJECT TERMS (Continue on reverse if necessary and identify by block number)
FIELD	GROUP	SUB. GR.	Solar Plasma Propulsion;
21	08		Spectroscopy of Alkali Metal Vapors,
			Spectroscopy of Alkali Metal Hydrides, (see reverse)

19. ABSTRACT (Continue on reverse if necessary and identify by block number)

The simultaneous measurement of absorption and emission spectroscopy is proposed to enable quantitative determination of the performance of a gaseous plasma solar energy receiver.

Production of an experimental spectroscopy data base of species composed of hydrogen and selected Group 1 elements (the alkali metals) and Row 2 elements (carbon, nitrogen, and oxygen) approaching conditions heretofore unattained in a static gas spectrometer cell, 3000 K and 100 atmospheres, is the principal objective of the project.

Preliminary design specifications for a spectrometer cell with automated flow control, pressure control, and plasma composition control are worked out in this interim report. The window-to-window distance of the cell is ten to fifteen inches and the optical path is one to three inches. Keywords:

20. DISTRIBUTION/AVAILABILITY OF ABSTRACT	21. ABSTRACT SECURITY CLASSIFICATION
UNCLASSIFIED/UNLIMITED ☒ SAME AS RPT. ☐ DTIC USERS ☐	Unclassified

22a. NAME OF RESPONSIBLE INDIVIDUAL	22b. TELEPHONE NUMBER (Include Area Code)	22c. OFFICE SYMBOL
Wayne E. Roe	(805) 275-5346	XRX

DD FORM 1473, 83 APR   EDITION OF 1 JAN 73 IS OBSOLETE.

Block 3 Cont'd

March 1987; other requests for this document must be referred to AFRPL/TSTR (STINFO), Edwards Air Force Base, California 93523-5000

Block 18 Cont'd

Lithium Vapor; Lithium Hydride; Sodium Vapor; Sodium Hydride; Potassium Vapor, Potassium Hydride; Rubidium Vapor; Rubidium Hydride; Cesium Vapor, Cesium Hydride, Rhenium Furnace; Rhenium Thermocouple; Plasma Spectroscopy; Blackbody Receivers, Radiant Energy Transfer; Spectroradiometry; Radiation Trapping; Solar Thermal Propulsion; Laser Propulsion.

Accesion For	
NTIS CRA&I	☐
DTIC TAB	☑
Unannounced	☐
Justification	
By	
Distribution /	
Availability Codes	
Dist	Avail and / or Special
C-2	

TABLE OF CONTENTS

LIST OF ILLUSTRATIONS

SECTION 1

INTRODUCTION

The use of a solar-powered propulsion system with a hydrogen propellant for missions beyond low earth orbit can significantly increase payload over the use of a chemical propulsion system, and can significantly reduce travel time over the use of an ion or electric propulsion system. Further, with the available low-density solar power in space, about 0.15 watts per square centimeter, there is no need to carry an independent power source aboard the spacecraft. Thus, solar-powered hydrogen propulsion circumvents the limitations imposed on the payload of low specific-impulse chemical systems and the travel time of low-thrust electric systems, and fills the undesirable gap in current propulsion technology.

Several schemes have emerged for converting the radiant energy of the sun into the internal energy of the hydrogen propellant. Their common feature involves the concentration of low-density solar energy by a factor approaching ten thousand. Two basic kinds of receiver device to absorb and transfer concentrated radiant energy to hydrogen have been proposed: (a) blackbody receiver and (b) plasma receiver.

The theoretical properties and engineering principles of blackbody receivers have been extensively enumerated.[1] Radiant energy is absorbed on solid surfaces and energy is conducted through the absorbing surface to the hydrogen propellant. The maximum operating temperature of blackbody receivers is limited by materials of construction. The maximum efficiency for a blackbody receiver with perfect aspect ratio (diameter/length = 0) is defined by

$$\eta = 1 = E_r/E_o, \qquad (1)$$

were E_o is the input energy flux, and E_r is the reradiated energy flux, which depends only on the operating temperature, T_b, and which is given by the

---

[1]Kreith, F., <u>Radiation Heat Transfer for Spacecraft and Solar Power Plant Design</u> (International Textbook Company, Scranton, PA, 1962).

1

Stefan-Boltzman law:

$$E_r - \sigma T_b^4. \qquad (2)$$

With a plasma receiver, concentrated radiant energy is absorbed directly by a hydrogen gas and seedant mixture. Seedant material provides the various species required to absorb the radiant energy of the solar spectrum, and energy is transferred to the hydrogen propellant by collisions with hot, optically excited seedant species.

One of the two principal motivations for developing a plasma receiver is the ability to manipulate the plasma geometry and thermal structure through flowfield engineering that would protect the materials of construction from the hot plasma core with a layer of colder propellant. Although the maximum operating temperature of blackbody receivers is restricted to temperatures below about 3000 K by the limitations of currently available refractory materials, the maximum operating temperature of a plasma absorber is considerably less restricted.

The second principal motivation for developing a plasma receiver[2] derives from the considerably reduced losses by reradiation from a thermally structured plasma. Energy that would otherwise be lost from the hot plasma core by reradiation is reabsorbed by the surrounding cooler gas.

This potential superior performance of the plasma receiver (higher temperature and lower reradiation loss) needs to be optimized against the amount of seedant required to support a given amount of radiant energy absorption. The specific impulse (I_{sp}) of a propellant composed of hydrogen and seedant is the mass-weighted average of the specific impulses of the various species; the I_{sp} of a species is inversely proportional to the square root of the species' molecular weight. Thus, use of excessive amounts of seedant, or use of high-molecular-weight seedants, could degrade specific impulses to levels lower than those already achievable with a simpler blackbody receiver.

---

[2]Forward, R, "Alternate Propulsion Energy Sources," AFRPL-TR-83-067, December 1983.

2

SECTION 2

PROGRAM OBJECTIVE

The principal objective of this research is to determine the emission and absorption spectroscopy of mixtures of hydrogen and minimal quantities of seedants. The experimental design will enable acquisition of emission and absorption coefficients up to the limits of currently available refractory materials, approaching 3000 K and 100 atmospheres.

One of the most novel accomplishments of this research will be the production of a state-of-the-art plasma spectroscopy cell (PSC) with the capability to control temperature, pressure, and composition to extremes that have not been achieved before. Chemical physics researchers, especially spectroscopists and kineticists, would be enthusiastic about extending their research into these new regimes. Perfection of the high-temperature facility required to accomplish the objective of this program would prepare their way. The concluding remarks of Nelson's paper[3] contain a strong message to motivate the research of this program:

> "...there is a massive lack of knowledge and understanding in a temperature region that is limited mostly by lack of ingenious experimentation--most often by the containment problem. There are techniques at hand today, however, for the bold experimenter to enter this region and unfold a tale that should excite all scientists, whether their inclinations are theoretical, experimental, fundamental, or technological. The main requirements are imagination and a willingness to depart from preconceived notions of how chemical studies at extreme temperatures should be carried out."

---

[3]Nelson, L.S., Advances in High-Temperature Chemistry 4, 171-236 (1971).

SECTION 3

BACKGROUND

The solar plasma receiver was first conceived and analyzed by researchers at the University of Washington. Applications in propulsion, thermal electric energy conversion, and magnetohydrodynamics have been described. Parametric studies of radiant energy deposition in a gas flowing in the direction of radiant energy propagation were carried out for various model gas spectra.[4-7]

Solutions of an approximate energy balance equation were studied in a one-dimensional model described by

$$\partial(C_p \, T \, \rho_o \, U_o)/\partial x = A(x) - R(x), \qquad (3)$$

where the right-hand side, the incremental energy input at point x, is a function of heat capacity, C_p, temperature, T, density, ρ_o, and flow velocity, U_o of the gas. The absorbed and radiated energy at point x, $A(x)$ and $R(x)$, respectively, is calculatable from the emission and absorption spectra of the gas, i.e., from the emission and absorption coefficients. The nonlinear Equation (3) was solved iteratively until $\partial T/\partial x$ converged to a stable function of T, which enabled calculation of the maximum temperature, T_{max}, and the efficiency, η_{plasma}, of the solar plasma receiver charged with a gas of given specified hypothetical spectroscopy.

Figure 1 compares the efficiencies of a blackbody receiver and solar plasma receivers charged with various model gases, including potassium vapor at 1-atmosphere pressure, and red, blue, and gray gases. The input radiant energy

[4]Mattick, A.T., Hertzberg, A., Decher, R., and Lau, C.V., "High Temperature Solar Photon Engines," Journal of Energy 3 (1) 30-39 (1979).

[5]Mattick, A.T., "Coaxial Radiative and Convective Heat Transfer in Gray and Nongray Gases," Journal of Quantitative Spectroscopy and Radiation Transfer 24 (4) 323-334 (1980).

[6]Rault, D.F.G., and Hertzberg, A., "Radiation Energy Receiver for Laser and Solar Propulsion Systems," AIAA/SAE/ASME 19th Joint Propulsion Conference, paper AIAA-83-1207, 8 pages.

[7]Rault, D.F.G., "Radiation Energy Receiver for Solar Propulsion Systems," Journal of Spacecraft 22 (6) 642-648 (1985).
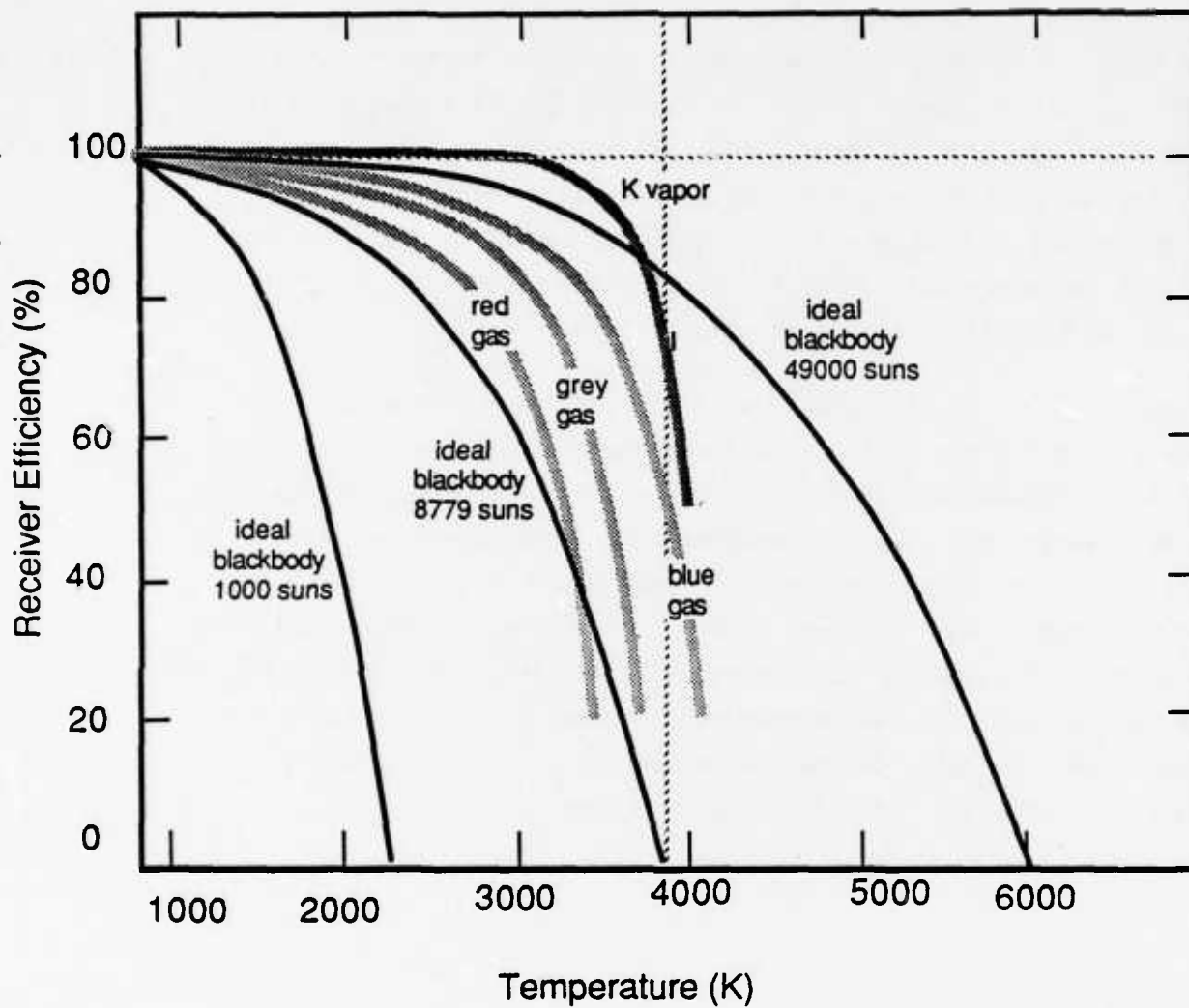
Figure 1. Efficiencies of Blackbody and Various
Solar Plasma Receivers

5

is concentrated by a factor of 8779 in these calculations, and reradiation trapping is predicted for all of the plasma receivers. Also, T_{max} for the potassium and blue gas receivers is greater than the maximum T_b achievable in the blackbody receiver.

Radiation trapping in the plasma receiver is analogous to the Earth's greenhouse effect. The thermally structured absorber gas is transparent to a portion of the solar spectrum in its outside cooler layers so that energy penetrates to the hot core where the plasma is optically thick to all wavelengths, and absorption is completed. The amount of radiation trapping depends on the details of the spectroscopy and its temperature dependence, which ultimately determines the thermal (spatial) structure of the plasma.

Figure 2 shows the absorption spectrum of a hypothetical blue gas which transmits most of the sun's blue light at low temperature and which becomes optically thick to all wavelengths at high temperature. Radiation trapping in the blue gas is greater than in others because blue light penetrates the cooler outside layers to the hot core, whose higher temperature is maintained by absorption of blue radiation. The core is optically thick, so its reradiation approximates a blackbody spectrum characterized by the core temperature, T_{max}. The core reradiation, which is red-shifted relative to the input, 6000 K incident solar radiation, is reabsorbed by the cooler surrounding gas, which is optically thick only to these red-shifted wavelengths.
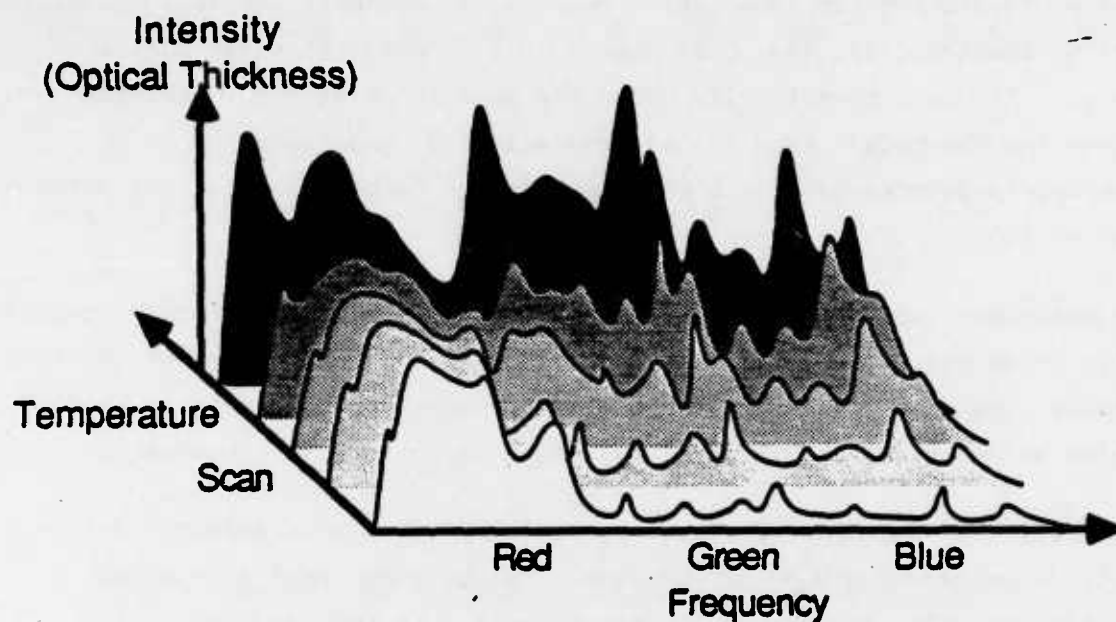
Figure 2. <u>Temperature Dependence of Absorption Spectrum of Hypothetical Blue Gas</u>. The gas is optically thick to red light at low and high temperatures. The optical thickness to blue light increases from a low value at low temperature to a high value at high temperature. This is the general feature of the spectrum of gases with the maximum capability for radiation trapping.

SECTION 4

GENERAL EXPERIMENTAL APPROACH

The experiment that produces the temperature, pressure, and composition dependence of the emission and absorption spectroscopy of hydrogen and seedant mixtures would provide the information required to evaluate the $A(x)$ and $R(x)$ quantities, Equation (3), that must appear in all models of solar plasma propulsion. Figure 3 symbolically shows the dynamic relationship between the experiment and the models, and illustrates a typical experiment where spectroscopy is determined over a wide temperature range at a constant pressure and composition.

The experiment would make use of a wavelength-scanning spectrometer capable of acquiring emission and absorption spectra on a millisecond time scale. The spectrometer would be assembled around a high-temperature, high-pressure cell into which hydrogen and seedant mixtures could be introduced and observed.

Fabrication of a plasma spectroscopy cell (PSC), an apparatus to confine a well-defined column of gas in an observable hot zone at temperatures and pressures approaching 3000 K and 100 atmospheres, has been proposed. As conceived, the idealized hot zone would contain the chemically, thermally, and radiatively equilibrated gas; radial and axial temperature and composition gradients in the hot zone would be negligible, and the optical path length would be well defined. Ideally, the hot zone would approach a perfect blackbody cavity whose equilibrium and uniformity would be minimally perturbed by observation.

Preliminary parametric studies of the relationships between flow and gradient development have shown that the achievement of the idealized hot zone can be approached by flow control alone, so that spectroscopic information can be acquired independently of the kinetics and transport issues. Thus, reaction times are much smaller than the characteristic diffusion times for energy, mass, and momentum transport, and flow may be manipulated to control the latter.

Mattick's 1-Dimensional Model

Experimental Spectroscopy

|←——— optically thick ———→|

→| optically thin |←

T_0 T_1 T_2 T_3 T_4 T_5

264 Suns

8,779 Suns

1200 K   2800 K 3200 K

Measurements on
optically thin slice

FLOW ——————→

P = 1 atm   Y = pure Potassium

$\partial/\partial x \, (T \, Cp \, \rho \, Uo) = A(x) - B(x)$

cell

absorption spectrum

emission spectrum

T_0
T_1
T_2
T_3
T_4
T_5

Constant P
Constant Y

Scan T

A(x)

R(x)

BASIC
RESEARCH
SPIN-OFFS

2-Dimensional Model of Solar Plasma Thruster

Hydrogen

10,000 Suns ——→

1,000 Suns ←——

window

1200 K   3800 K

Seedants

Figure 3. Diagram Symbolizing the Relationships Between the
Models and the Proposed Experimental Spectroscopy
Where Temperature is Ramped at Constant Pressure and
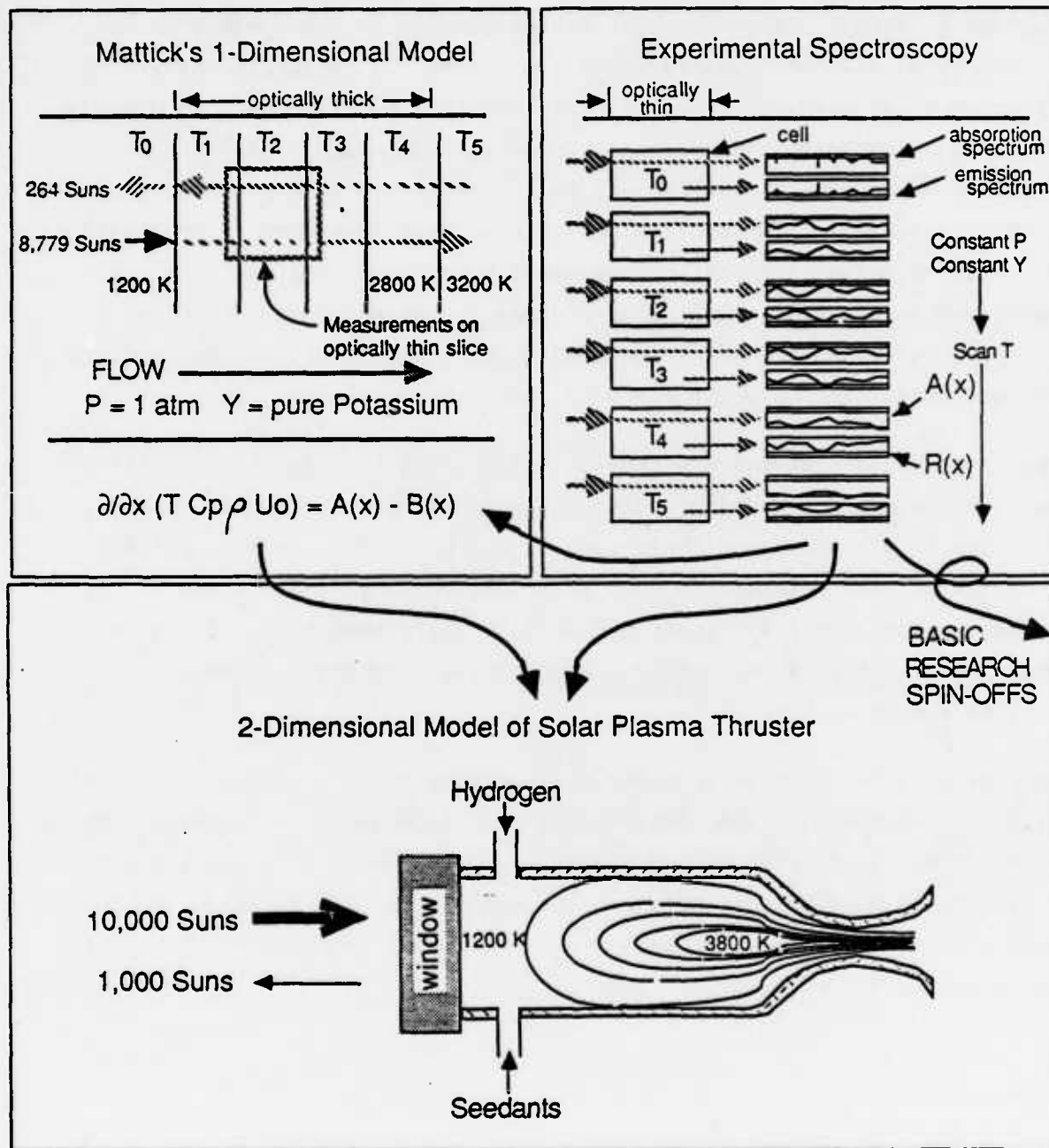Composition.

9

4.1 Candidate Seedants

The candidate seedants suggested for solar plasma rocket propulsion have
been confined to alkali metal vapors, to the exclusion of other elements.[8],[9]
All of the pure alkali metal vapors exhibit rich absorption spectroscopy that
arises from numerous kinds of spectroscopic transitions in monomer and dimer
species. This spectroscopy is currently under intense experimental and
theoretical investigation[10],[11] by groups whose objectives include discovery of
spectroscopic transitions for application in new laser development, applications
of alkali metal plasmas in magnetohydrodynamic technology, and definition of
performances of pure alkali metal vapor plasmas in the absorption of solar
energy. The experiments have been confined to pure alkali metal vapors and to
temperatures approaching only about 1400 K, and subatmospheric pressures.

Indeed, the Group 1 elements of the periodic table (Li, Na, K, Rb, Cs) have
the lowest ionization potentials, so strong photoionization transitions and high
concentrations of electrons and ionic species are produced upon absorption of
visible radiation. Notwithstanding its rich spectroscopy in the visible, the
gain in specific impulse realized by use of a strongly absorbing heavy alkali
metal would be counteracted by degraded specific impulse from increased
propellant molecular weight.

To the extent that species composed of lightweight Row 1 elements (Li, Be,
B, C, N, O, F, Ne) exhibit rich spectroscopy, Row 1 seedants would be winning
candidates for use in a solar plasma thruster. Also, Row 1 elements are prime
seedant candidates because they provide expanded flexibility in tailoring the
spectrometry of the hydrogen and seedant mixture, which is required to maximize
radiation trapping and receiver performance.

---

[8]Forward, Op. Cit.

[9]Perry, F.J. "Solar Thermal Propulsion, An Investigation of Solar Radiation
Absorption in a Working Fluid," AFRPL-TR-84-032, June 1984.

[10]Stwalley, W.C., and Koch, M.E., "Alkali Metal Vapors: Laser Spectroscopy and
Applications," Optical Engineering 19 (1) 71-84 (1980).

[11]Gole, J.L. and Stwalley, W.C., "Metal Bonding and Interactions in
High-Temperature Systems with Emphasis on Alkali Metals," American Chemical
Society Symposium Series, 179 , ACS, Washington, D.C. (1982).

4.2 Experimental Protocol-Temperature Scan

A typical experiment, where the temperature dependence of the spectrometry of a fixed-pressure, fixed-composition hydrogen and seedant mixture is measured, would proceed as follows. Flows to establish composition and pressure would be set up at an initial low temperature, and the spectrometer would be set to scan and record emission and absorption spectra.

The temperature would be ramped, over a period spanning several minutes, from about 1000 K to about 2800 K. The plasma would appear in vivid colors, perhaps undergoing dramatic color changes as its gross average optical thickness increases with the rising temperature. The data acquired would consist of spectroscopy on generally optical thin layers of a uniform plasma, which would be used as A and R, Equation (3), input for a model that computes the performance of a thermally structured plasma.

4.3 Optical Path Length of Cell

It is not within the scope of this research project to engage in design of operational solar receivers for solar propulsion applications. That is left as an exercise for the propulsion engineering community. The sizing criterion for the optical path length of the spectrometer cell is based on the practicable limitation expected in the size of a generic[12] solar plasma receiver. Hydrogen and seedant mixtures that absorb 95% of incoming solar radiation over a distance of one meter would be identified as candidates for use in solar plasma propulsion. Thus, by the Beer-Lambert Law, the gross average absorption coefficient of candidate mixtures is 0.03 cm^{-1}.

The range of ideal measurements in absorption spectroscopy lies in the neighborhood of 7 to 20% absorption, which is a limit defined by the trade-off between minimizing optical thickness and maximizing the absorption and emission signals. Candidate mixtures with absorption coefficients of 0.03 cm^{-1} absorb 7 to 20% over absorption paths between 2.4 and 7.4 cm. Inasmuch as the range of temperature, pressure, and composition to be investigated in this research is broad, orders of magnitude variations in the wavelength-dependent absorptivities

---

[12]Shoji, J. M., "Solar Rocket Component Study," AFRPL-TR-84-057.

11

are expected. A spectrometer cell with a variable path up to about 7.5 cm maximum would enable acquisition of reliable spectroscopic data that span the conditions from optically thick to absorptions with coefficients in the neighborhood of 0.004 cm^{-1}.

4.4 Spectroscopy Parameter Space

Figure 4 shows the extent of the measurable parameter space in a cell with an optical path length between 2.5 and 7.5 mm. Measurable absorption cross sections approach 10^{-6} Å^2 as the density of absorbing species approaches 10^{21} cm^{-3} (100 atm at 1000K). Thus, spectroscopic transitions with absorption cross sections ranging over nearly eight orders of magnitude will be measurable.
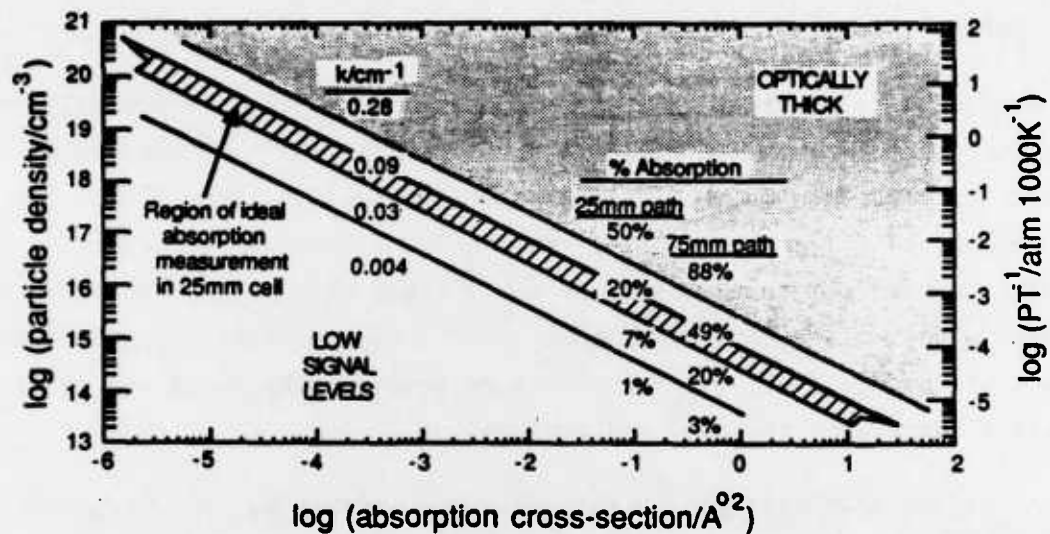
Figure 4. <u>Diagram Showing the Parameter Space in a Plasma Spectroscopy Cell</u>. A species with a particle density of 10^{15} cm^{-3} and an absorption cross section between 0.3 and 0.8 Å^2 would produce an ideal absorption signal between 7 and 20% in a 25-mm cell.

SECTION 5

DETAILED PRELIMINARY DESIGN

Figure 5 shows the conceptual layout of the key element of the experimental hardware, a vacuum-insulated, high-temperature, high-pressure plasma spectroscopy cell, PSC. Not pictured are the flow control subsystem, the vacuum system, the spectrometer, and the data acquisition and reduction system.

5.1 Refractory Metals Engineering

Production of free-standing refractory metal objects, especially rhenium objects,[13],[14] has been perfected sufficiently to enable production of a furnace capable of reaching 3000 K. Detailed design specifications for such a furnace may be derived from creep rupture testing[15] and hydrogen permeability studies carried out on a variety of small tubes made from rhenium and alloys of rhenium with tungsten and molybdenum. Pure rhenium tolerates the greatest amount of thermal cycling; it is least permeable to hydrogen and has the greatest resistance to creep and rupture.

Rhenium compatibility with the seedant materials has not been studied, so this experiment will provide information in this area. Harding, Tuffias, and Kaplan[16] have described the remarkable oxidation resistance of rhenium, coated with an ultrathin layer of irridium deposited by chemical vapor deposition. The expectation is that seedant and rhenium compatibility will not impact significantly on the operation of the PSC and any high-temperature corrosive process encountered would be designed to occur in areas not likely to lead to furnace failure.

---

[13]Kaplan, R. and Tuffias, R., "Fabrication of Free Standing Shapes by Chemical Vapor Deposition," Proceedings of the International Symposium on Electroforming/Deposition Forming, Los Angeles, CA, March 1983.

[14]Tuffias, R., Garg, A., and Kaplan, R., "Chemical Vapour Deposition in Joining Refractory Metals," International Journal of Refraction and Hard Metals 3, (4) (1984).

[15]Svedberg, R.C., "Hydrogen Permeability Through Re and Mo-Re Alloy With and Without Chemically Vapor-Deposited Tungsten Coatings," Thin Solid Films 72, 385-392 (1980).

[16]Harding, J.T., Tuffias, R.H., and Kaplan, R.B., "High Temperature Oxidation Resistant Coatings," AFRPL-TR-84-035, June 1984.
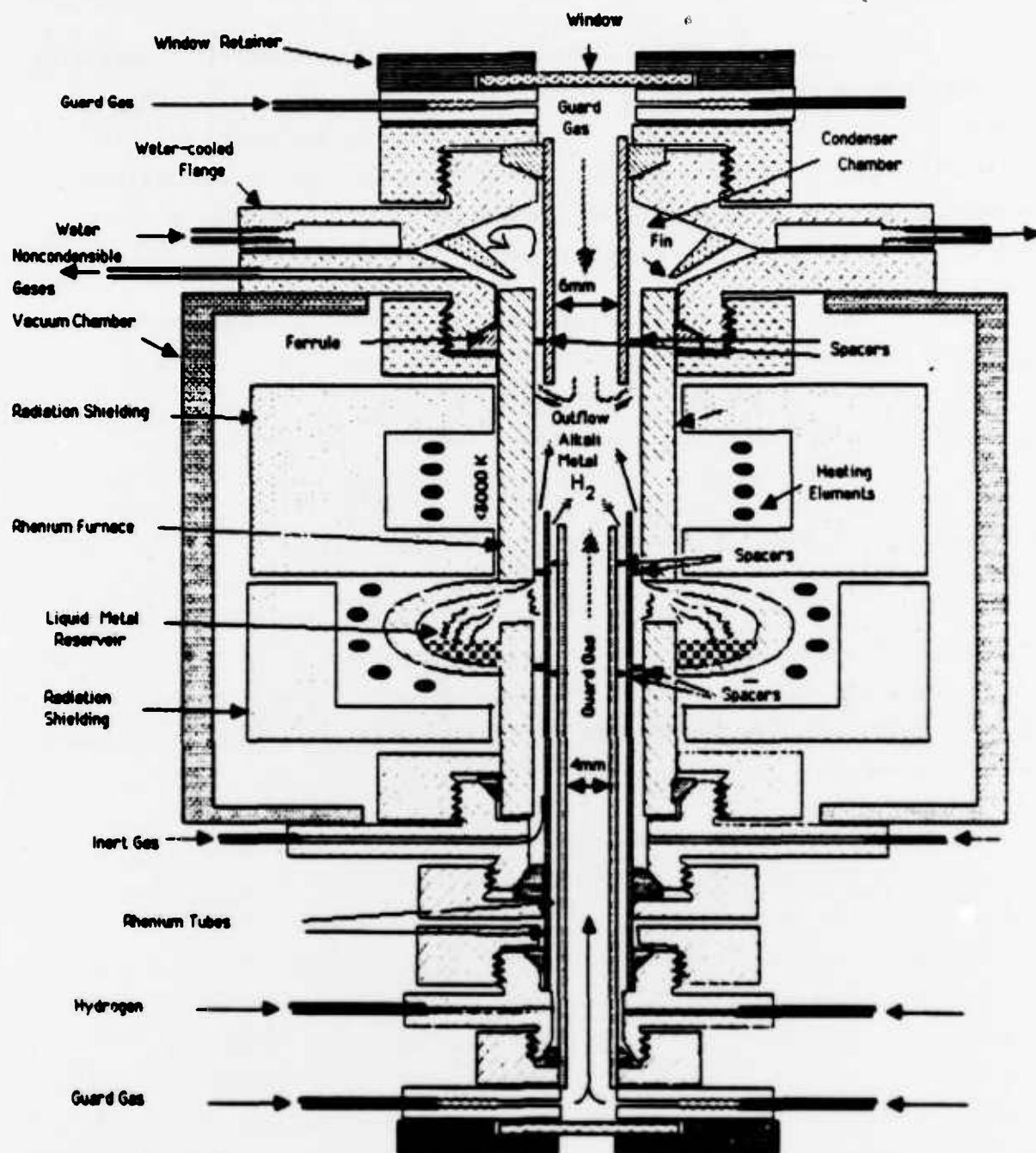
14

Figure 5. Layout of Plasma Spectroscopy Cell.

5.2 Vacuum Insulation and Cell Optics

For a high-temperature furnace, vacuum insulation and radiation shielding are the most effective means of establishing the large temperature gradients required to position viewing windows close to the high-temperature cavity. Shorter distances between the plasma cavity and the window produce better viewing optics. For example, a 6-mm-diameter cell with a window-to-cavity distance of 120 mm has an "f-number" of 20.

Svedberg[17] described a high-performance, cup-shaped, 45-layer radiation shield (for insulation of artificial heart power sources) that is capable of maintaining a temperature gradient of 500 K per 5 mm. This vacuum foil insulation has been used in the construction of a cylindrical muffle furnace (40 cm by 13 cm diameter) that reaches 2100 K with only 1500 watts of power.

5.3 Plasma Spectroscopy Cell With Concentric Flows

The details of the PSC shown in Figure 5 are described in the paragraphs below. All refractory metal parts are made as one-piece tubes, and O-ring or ferruled seals are made external to the high-temperature and high-vacuum system. Thus, disassembly and removal of the internal parts may be undertaken without breaking vacuum.

With the concentric tube arrangement, two reactive gases enter the hot zone in laminar flow annular sheaths that surround the cylinder of guard gas. The spectroscopy of the static, equilibrium mixture of test gas will be measurable at a very low flow where the time scale for diffusive mixing and reaction is much shorter than the flow time. In regimes of higher flowrate, diffusion controlled structure along the boundaries of the gases should be observable. The flowfield would be similar to a diffusion flame, so modeling with a two-dimensional flow model would be appropriate for high-flow experiments. Numerous alternative complicated and interesting flow geometries could be created in the hot zone by admitting the various gases at unequal linear velocities. Also, reactive gas may be substituted for guard gas, and one or more of the entering gases may be pulsed.

---

[17]Svedberg, R.C., "On the 10-Year Static Vacuum Integrity of Vacuum Foil Insulation for an Implantable Artificial Heart," J. Vac. Sci. Tech. 11 (4) 806-812 (1984).

5.4 Flow System

Figure 6 shows the flow system design, and Figure 7 shows the flow and diffusion parameter space based on 10 cm^3 min^{-1} at STP (sccm) flow of argon guard gas through a 4-mm-diameter guard gas tube. The internal tube dimensions of the concentric tubes (4.0, 5.7, and 6.9 mm ID) are designed to produce equal linear velocities through the three channels when the volumetric flowrates are equal.

A separate channel for admitting reactive gas is included in this design to permit the study of candidate seedants in the first row of the periodic table that could not be substituted for a guard gas because they would begin exhibiting spectroscopy in the hotter regions of the tube carrying the light beam. Inclusion of the reactive gas channel will permit evaluation of carbon, nitrogen, and oxygen seedants (by metering of methane, ammonia, or water into the middle annular space).

Gas leaves the hot zone through a fixed annular space between the furnace wall and a rhenium tube that carries guard gas and the light beam. Condensible products plate out in a heat exchanger and condenser cavity. The pressure drop from hot zone pressure (up to 100 atmospheres) to atmospheric pressure occurs downstream of the exit pressure controller, where the exit gases have cooled to ambient temperature.

5.5 Flow and Diffusion Parameter Space

Figure 7 shows the pressure and temperature dependence of the flow characteristics and its relation to the diffusion coefficient's pressure and temperature dependence. The average diffusion distance in time t is approximately $(2D_{AB}t)^{\frac{1}{2}}$, so that doubling of mass flows through the input channels at constant pressure produces an approximately constant value of the ratio of linear velocity to the diffusion velocity as the temperature increases from 1000 K to 3000 K. The ratio may be controlled by fixing the mass flow at a value that depends on the channel diameter and a characteristic diffusion distance.

17
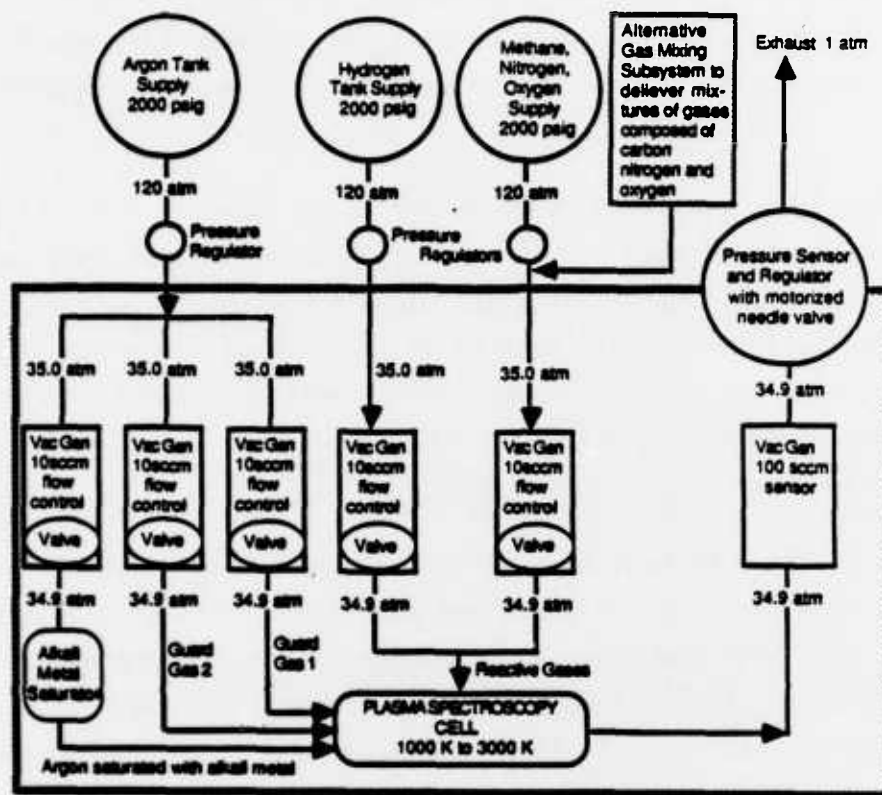
Figure 6. _High-Pressure Programmable Flow Control System._
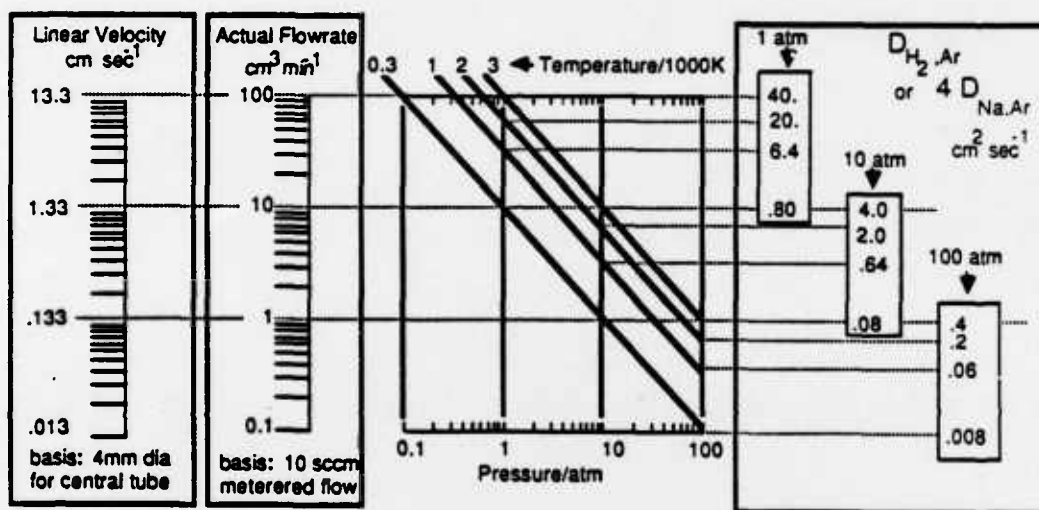
Figure 7. <u>Flow and Diffusion Parameter Space.</u> Nomogram
showing the temperature and pressure dependence
of the volumetric flowrate and linear velocity
of a gas metered at 10 sccm through a 4mm ID
tube. The pressure and temperature dependence
of the binary diffusion coefficients is also
indicated. Thus, at 3000 K and 1 atm, the
diffusion coefficient is 40 cm^2 sec^{-1}, which is
slightly less than the flow velocity of 13 cm
sec^{-1}.

5.6 Heat Transfer and Cooling Requirements

Heat transfer from the hot zone to the cool windows and O-ring seals by conduction through the rhenium furnace body and tubes exceeds, by two or more orders of magnitude, radiant heat transfer, heat transfer by conduction through the gases, and convective heat transfer to the outlet condenser forced by flow.

Conductive heat transfer through the furnace body will amount to a maximum of approximately 1500 watts based on a 5-mm wall thickness for the furnace body, and a temperature gradient of 1000 K cm^{-1} between the hot zone and ambient temperature.

SECTION 6

MODELING

6.1 Modeling the Zero-Dimensional Problem

The modeling of the zero-dimensional problem, (i.e., the static, equilibrium plasma gas), may be carried out with the CHEMKIN code recently installed in the RPL VAX/VMS system. The thermodynamic data base for the various species that will be created within the plasma cavity needs to be expanded and updated continuously. The latest issue of the NASA thermodynamics data base should be acquired and supplemented as required by the modeling for this project. Thus, equilibrium composition of a test gas mixture within the plasma cavity will be calculatable from any given specification of initial conditions, i.e., temperature, pressure, and input gas composition.

6.2 Modeling the One-Dimensional Problem

The one-dimensional model consists of a flowing gas with a given incident solar radiation field of around 10,000 suns. The gas is in chemical equilibrium, but a thermal structure develops along the one-dimensional axis as a result of the flow and the temperature dependence of the spectrometry of the gas.

A modified form of the model developed by Mattick[18] would be developed before and during the experimental work on this project. Mattick described the behavior of certain gases with model absorption spectra, but the temperature dependence of the spectrometry was not an independent variable. Rather, efficiency and one-dimensional thermal structure were computed as a function of the optical thickness of the gas; flow and thermal dependencies were investigated.

---

[18]Mattick, A.T., Op. Cit.

21

6.3 Modeling the Higher-Dimensional Problems

The higher-dimensional problems, one-dimensional with chemical reaction or diffusional flow, or two-dimensional with chemical equilibrium, are at least an order of magnitude more expensive than the modeling proposed above. The one-dimensional reactive flow model is currently being exercised at RPL.

Merkle and his associates[19] have described a two-dimensional flow model that simulates the interaction of an intense laser radiation field with a hypothetical absorber gas. Inclusion of temperature-dependent spectroradiometry (with chemical equilibrium) in Merkle's model would greatly increase its complexity. Addition of diffusion or chemical disequilibrium to this two-dimensional, variable spectroradiometry model would be appropriate to its development.

---

[19]Molvik, G.A., Dochul Choi, and Merkle, C.L., "A Two-Dimensional Analysis of Laser Heat Addition in a Constant Absorptivity Gas," AIAA 23, 1053-1060 (1985).

SECTION 7

CONCLUSIONS AND IMPLEMENTATION OF PLAN

The goals of this project may be accomplished during three sequential periods in which the following milestones would be achieved. First period: fabrication of the plasma spectroscopy cell and its calibration, including diagnostic testing by spectroscopic measurements of the well known, low-temperature alkali metal spectroscopies; second period: acquisition of spectroscopic information about hydrogen and seedant mixtures; third period: finalization of models and interpretation of results.

Final design and fabrication of the spectroscopy cell will be accomplished in the first period. At the end of the first period, breadboard spectroscopy will be undertaken with existing hardware wherever possible, and experimental spectroscopic diagnostics of system performance will be developed. The zero-dimensional model will also be developed by the end of the first period.

During the second period, a commercial spectroradiometer will be acquired, or a custom instrument will be designed and constructed. The spectroscopy of hydrogen and seedant mixtures will be determined as a function of temperature, pressure, and composition. The development of an extended one-dimensional (chemical equilibrium) model will be undertaken and interfaced with the experiment to provide real-time prediction of solar plasma receiver performance.

During the third period, results will be analyzed and interpreted, and development of the two-dimensional (chemical equilibrium) model will be undertaken. An assessment of future experimental work will be made and priorities for development of higher dimensional models (one- or two-dimensional with chemical or diffusional disequilibrium) will be established.